

## The Belle II Experiment

---

**Carlos Marinas**<sup>\*†</sup>

*University of Bonn*

*E-mail:* [cmarinas@uni-bonn.de](mailto:cmarinas@uni-bonn.de)

The Belle II experiment at the asymmetric  $e^+e^-$  SuperKEKB collider is a major upgrade of the Belle experiment, which ran at the KEKB collider at the KEK laboratory in Japan. The design luminosity of SuperKEKB is  $8 \times 10^{35} \text{ cm}^{-2}\text{s}^{-1}$ , which is about 40 times higher than that of KEKB. Commissioning of the main ring of SuperKEKB has started in February 2016 and Belle II is expected to accumulate an integrated luminosity of  $50 \text{ ab}^{-1}$  well within the next decade. The experiment will focus on searches for new physics beyond the Standard Model via high precision measurements of heavy flavor and searches for rare signals. To reach these goals, the accelerator, detector, electronics, software, and computing systems are all being substantially upgraded. In this talk we present the status of the accelerator and of the different Belle II sub-detector upgrades.

*XXIV International Workshop on Deep-Inelastic Scattering and Related Subjects*

*11-15 April, 2016*

*DESY Hamburg, Germany*

---

<sup>\*</sup>Speaker.

<sup>†</sup>The Belle II Collaboration.

## 1. SuperKEKB

The  $B$ -Factory experiments BaBar and Belle helped successfully establishing many aspects of the Standard Model of particle physics [1], such as the first observation of Charge-Parity ( $CP$ ) violation outside the kaon system, the precision measurements of the CKM parameters  $V_{ub}$  and  $V_{cb}$ , and the measurement of rare  $B$ -meson decays potentially sensitive to physics processes beyond the Standard Model. Their measurements were an important contribution to establish the CKM picture of  $CP$  violation, leading to the Nobel prize in physics for Kobayashi and Maskawa in 2008. The Belle II experiment was conceived as a successor to increase the measurement sensitivity by an order of magnitude and to search for signs of new physics in rarer processes. The data set needed to achieve these physics goals requires an integrated luminosity of  $50 \text{ ab}^{-1}$  [2]. The design peak luminosity  $8 \times 10^{35} \text{ cm}^{-2} \text{ s}^{-1}$ , 40 times larger than the world record achieved by its predecessor KEKB, makes it necessary to upgrade and modernize both the existing accelerator (KEKB) and the detector (Belle). The new accelerator (SuperKEKB) will collide electrons and positrons inside the Belle II detector at a centre-of-mass energy of 10.58 GeV using asymmetric beam energies to produce a boost in the laboratory frame. At this energy a short-lived bound state of two  $b$ -quarks, the  $\Upsilon(4S)$  resonance, may form, which decays nearly uniquely into  $B$ -meson pairs.

## 2. Belle II

The new Belle II detector is a specialized multilayer particle detector. It covers a large solid angle, possesses a precise vertex reconstruction and momentum determination, good pion-kaon separation, and excellent measurement of the deposited electromagnetic energy. The ultra high luminosity implies also higher backgrounds and higher event rates, and therefore the new detector is also required to fully exploit the increased number of events and provide high precision measurements in this harsh environment. The new detector includes a vertex detector with two pixel and four strip layers, a drift chamber with long lever arm and small cells, a particle identification Cherenkov system, a fast electromagnetic calorimeter and a muon detector.

### 2.1 The Vertex Detector

The asymmetry of the colliding beam energies makes lifetime measurements possible, which is an important ingredient to observe  $CP$  violation in  $B_0\bar{B}_0$ -pairs. The essential observable is the lifetime difference which translates into a difference of decay lengths of the order of  $150 \mu\text{m}$ . Experimentally both  $B$ -meson decay vertices have to be separable, requiring an excellent impact parameter resolution. To cope with the increased event rate and provide the necessary high track resolution to reconstruct  $B$ -meson decay vertices, a new silicon vertex detector (VXD) is being built (Figure 1). The VXD [3] is composed of two systems: a four layer double sided strip detector (SVD) [4] at higher radii around the beam-pipe and a double-layer DEPFET-based pixel detector (PXD) [5] as the innermost sensing device.

One of the challenges of constructing the PXD is the increased rate of beam backgrounds and the expected high occupancy. In addition, the boost from the centre-of-mass to the laboratory system is reduced: the Lorentz factor  $\gamma\beta$  is a factor of two smaller at SuperKEKB in comparison to KEKB and to achieve the same physics performance the impact parameter resolution has to

improve by a factor of two with respect to the Belle experiment. To achieve this, two DEPFET-based pixel detector layers will be installed close to the interaction region at a radii of 14 mm and 22 mm, respectively. In order to minimize multiple scattering and the energy loss of particles crossing the detectors, the material budget has to be below  $0.2\%X_0$  ( $0.6\%X_0$ ) per layer for the PXD (SVD), including the sensors, readout electronics, support structures and services.

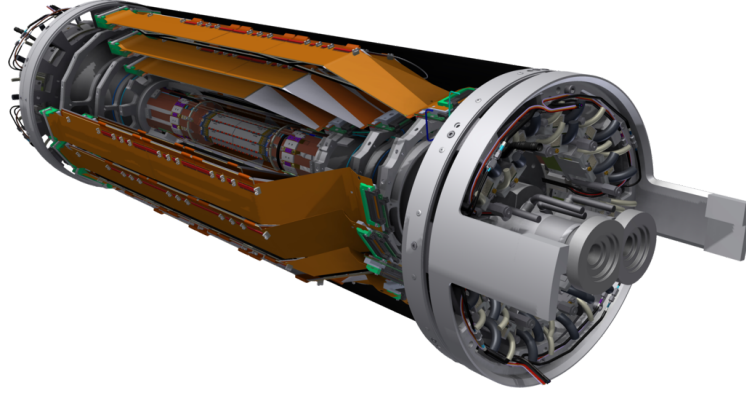


**Figure 1:** CAD drawing of the fully instrumented Belle II vertex detector. Closest to the interaction point, two layers of DEPFET-based pixel detectors followed by four layers of double sided silicon strip detectors.

The PXD sensors have pixel pitches ranging from  $50 \times 50 \mu\text{m}^2$  up to  $50 \times 85 \mu\text{m}^2$  that, together with SVD strip pitches from  $50\text{-}75 \mu\text{m}$  ( $160\text{-}240 \mu\text{m}$ ) on the p-side (n-side), results in a combined impact parameter resolution  $\sigma_{d0} \sim 15 \mu\text{m}$ .

## 2.2 Central Drift Chamber

Sitting just outside the inner detector systems, the Central Drift Chamber (CDC) is a gaseous detector that follows the barrel structure around the beam pipe. The Belle II CDC plays several important roles. First, it reconstructs tracks from charged particles and enables for momentum determination. It also provides particle identification using  $dE/dx$  energy loss within its volume. Finally, it provides trigger signals for efficient background reduction.

The detector is filled with a helium based gas mixture and, covering a maximum radius of 1200 mm, contains 15000 sense wires distributed in 56 layers. With this configuration and with sense wires of  $30 \mu\text{m}$  in diameter, the overall spatial resolution is  $\sigma_{r\phi} = 100 \mu\text{m}$ , the momentum resolution is  $\sigma_{p_T}/p_T \sim 0.3/\beta \oplus 0.1\% p_T$  (with  $p_T$  in GeV) and the track efficiency is expected to be above 95% for  $p_T > 0.5 \text{ GeV}$ . The resolution on  $dE/dx$  is 5% for minimum ionizing particles.

## 2.3 Time Of Propagation

Particle identification in Belle II [6] will be performed by combining information of the Time of Propagation (TOP) detector [7] in the barrel and of the Aerogel Ring Imaging Cherenkov (ARICH) [8] in the forward regions, together with the  $dE/dx$  in the CDC.

The TOP counter measures the emission angle of Cherenkov photons using time-of-propagation of the photons down a quartz bar to distinguish between kaons and pions. Each of the 16 TOP modules (Figure 2) contains two glued quartz bars (2.5 meters long, 2 cm thick), a forward mirror and an array of photodetectors for light detection on the backward region.

The quartz bars have to have a flatness better than  $6 \mu\text{m}$  over the complete length, a surface roughness better than  $0.5 \text{ nm}$ , bulk transmittance higher than  $98\%/m$  and a surface reflectance better than  $99.9\%$  per internal reflection.

The photodetectors are 32 units of  $4 \times 4$  micro channel plate photomultipliers that, with a gain of  $2 \cdot 10^6$  and a quantum efficiency higher than  $24\%$  possess a time resolution of  $35 \text{ ps}$ .

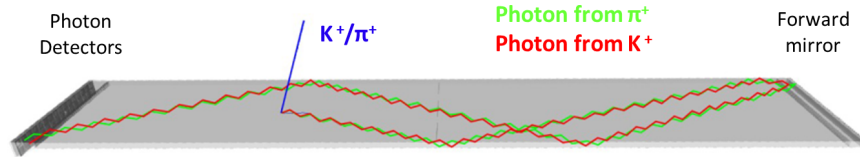


**Figure 2:** Sketch of one of the 16 quartz bars that are the Cherenkov radiator media of the TOP detector. Superimposed, the trajectories of the Cherenkov light emitted by charged kaons and pions.

## 2.4 Aerogel Ring Imaging Cherenkov

The particle identification in the forward endcap is performed via the ARICH, that provides  $K/\pi$  separation at  $>5\sigma$  confidence level at  $4 \text{ GeV}$ . The working principle of this detector is depicted in Figure 3. The detector is built from aerogel modules of two distinct types, with refractive index  $1.045$  and  $1.055$  and transmission length larger than  $40 \text{ mm}$ , and photodiodes to detect the emitted photons. Given this set of refractive indexes, the pion (kaon) threshold is  $0.44 \text{ GeV}$  ( $1.54 \text{ GeV}$ ) and the Cherenkov angle for a  $3.5 \text{ GeV}$  pion is  $307 \text{ mrad}$ .

The Cherenkov photon detection takes place using in total  $420$  hybrid avalanche photo detectors (HAPD), each segmented in  $144$  channels with  $5 \text{ mm}$  pitch cells. The gain is  $7 \cdot 10^5$  and the quantum efficiency for the interesting wavelength is larger than  $28\%$ .

With this detector configuration an angular separation of  $30 \text{ mrad}$  between pions and kaons is achieved at  $3.5 \text{ GeV}$ .

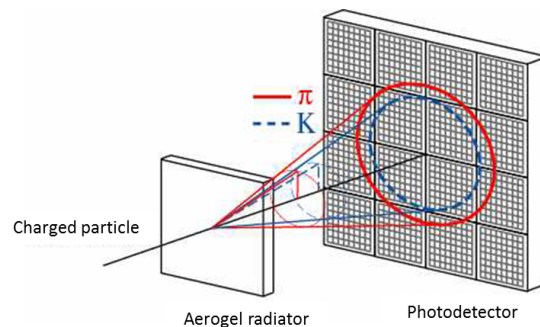


**Figure 3:** Working principle of the ARICH detector. For certain track parameters, the charged particle can emit Cherenkov light while traversing through the radiator. The cone light is detected at the photodetectors.

## 2.5 Electromagnetic Calorimeter

The main role of the electromagnetic calorimeter (ECL) [9] is to reconstruct the energy and angle of the photons and participate in the electron identification. In addition the ECL is used to provide the Belle II online luminosity measurement.

The ECL consists of a barrel and two endcaps of segmented arrays of CsI(Tl) [10] crystals with silicon photodiode readout. The photomultiplier gain is 255 and the quantum efficiency is larger than 25%. The signal is further processed by new electronics with waveform sampling capabilities for better disentangling the background from the signal using off-time cuts. The crystals are 30 cm deep resulting in  $16.1 X_0$  and the electromagnetic calorimeter energy resolution is 2% for 100 MeV photons.

## 2.6 Muon Detector

The last of the subdetector systems (KLM) [11] identifies  $K_L$  mesons and muons with high efficiency. The system consists of alternating layers of active counters and iron plates. In the barrel region, the active elements are resistive plate counters operating in limited streamer mode, like in the old Belle experiment. In the two innermost barrel layers and in both complete end-caps these modules have been replaced by scintillator strips to cope with the increased backgrounds. This scintillator strips have embedded wavelength shifter fibers guiding the light to multi-pixel photon counter detectors with a nanosecond time resolution placed at the end of the scintillator tiles.

## 3. Outlook

The new Belle II detector will be operated at the next generation of  $B$ -Factory experiments. The commissioning of the SuperKEKB accelerator has started in February 2016 and the physics data taking with the upgraded detector is scheduled by 2018.

## References

- [1] S. L. Olsen, arXiv:1601.01061 [hep-ex].
- [2] P. Urquijo, Nucl. Part. Phys. Proc. **263-264** (2015) 15. doi:10.1016/j.nuclphysbps.2015.04.004
- [3] G. Casarosa, PoS EPS -**HEP2015** (2015) 255.
- [4] K. Adamczyk *et al.* [Belle II SVD Collaboration], Nucl. Instrum. Meth. A **824** (2016) 406. doi:10.1016/j.nima.2015.09.076
- [5] M. Boronat Arevalo [DEPFET Collaboration], PoS VERTEX **2015** (2015) 014.
- [6] E. Torassa [Belle II PID Group Collaboration], Nucl. Instrum. Meth. A **824** (2016) 152. doi:10.1016/j.nima.2015.11.016
- [7] K. Matsuoka *et al.*, PoS PhotoDet **2015** (2016) 028.
- [8] S. Iwata *et al.*, PTEP **2016** (2016) no.3, 033H01 doi:10.1093/ptep/ptw005 [arXiv:1603.02503 [physics.ins-det]].
- [9] B. Schwarz [BELLE II calorimeter group Collaboration], PoS PhotoDet **2015** (2016) 051.
- [10] A. Aloisio *et al.*, Nucl. Instrum. Meth. A **824** (2016) 704. doi:10.1016/j.nima.2015.11.045
- [11] T. Ugllov, PoS PhotoDet **2015** (2016) 065.